

Article

# Event-Triggered Cooperative Predictive Control for Networked Multi-Agent Systems with Random Delays and Packet Dropouts

Zhonghua Pang , Tao Du, Changbing Zheng and Chao Li \*

Key Laboratory of Field Bus Technology and Automation of Beijing, North China University of Technology, Beijing 100144, China; zhonghua.pang@ia.ac.cn (Z.P.); dt1540561523@126.com (T.D.); cbzheng@mail.ncut.edu.cn (C.Z.)

\* Correspondence: lichao@ncut.edu.cn

**Abstract:** This paper addresses the cooperative output tracking control problem for a class of leader-following linear heterogeneous networked multi-agent systems subject to random network delays and packet dropouts in the feedback and forward channels of each agent. A state observer is established at the plant side of each agent, and an event-triggering transmission mechanism is introduced to decide which state estimate is transmitted to the corresponding controller so as to save the network resources of the feedback channel. To further compensate for the negative effects of those random communication constraints and the event trigger, a cooperative predictive control scheme with proportional and integral actions is proposed. Then, a necessary and sufficient condition is derived for the stability of the resulting closed-loop system. Finally, simulation results are given to show the effectiveness of the proposed scheme.



check for updates

**Citation:** Pang, Z.; Du, T.; Zheng, C.; Li, C. Event-Triggered Cooperative Predictive Control for Networked Multi-Agent Systems with Random Delays and Packet Dropouts. *Symmetry* **2022**, *14*, 541. <https://doi.org/10.3390/sym14030541>

Academic Editors: Jan Awrejcewicz, José A. Tenreiro Machado, José M. Vega, Hari Mohan Srivastava, Ying-Cheng Lai, Hamed Farokhi, Roman Starosta and Antonio Palacios

Received: 21 January 2022

Accepted: 5 March 2022

Published: 7 March 2022

**Publisher's Note:** MDPI stays neutral with regard to jurisdictional claims in published maps and institutional affiliations.



**Copyright:** © 2022 by the authors. Licensee MDPI, Basel, Switzerland. This article is an open access article distributed under the terms and conditions of the Creative Commons Attribution (CC BY) license (<https://creativecommons.org/licenses/by/4.0/>).

**Keywords:** networked multi-agent systems; cooperative tracking control; event trigger; network delays; packet dropouts

## 1. Introduction

In the last few decades, the cooperative control of networked multi-agent systems (NMASs) composed of multiple agents communicating with each other through networks has a very wide practical application in various fields, for example, satellite formation [1], multiple unmanned aerial vehicles [2], and mobile robots [3]. For example, in [3], multiple robots communicate through a connected undirected graph and then achieve a formation control to track a trajectory gradually. Most existing works focused on the cooperative output control of NMASs under ideal communication conditions [4–8]. However, in practical applications, the introduction of networks inevitably leads to communication constraints between multiple agents and within agents, such as random network delays and packet dropouts [9,10]. These communication constraints can not only affect system control performance but also seriously damage the closed-loop stability of NMASs.

Therefore, several control methods have been presented to deal with these communication constraints, such as the time-delay system method [11,12], robust control method [13], and stochastic control method [14]. In addition to the methods mentioned above, networked predictive control (NPC) is an effective approach to actively compensate for network communication constraints [15–22]. Furthermore, with accurate models of controlled plants, NPC methods can obtain almost the same control performance as that of the case without communication constraints. In [15–21], the output consensus problems of NMASs were investigated, where network delays were assumed to be constant. In [22], only random communication constraints in the feedback channel of each agent were considered. However, in practice, network delays and packet dropouts occur randomly due to bandwidth limitation and network congestion, and they also generally exist in both the feedback and forward channels, which thus motivate this study.

In addition, for NPC methods of NMASs in [15–22], a state observer is usually established and placed at the controller side of each agent, which thus needs to transmit a packet composed of multiple system outputs at the current time instant and previous time instants to the controller through the feedback channel of each agent. Moreover, due to the use of the time-triggered transmission mechanism, such a packet is needed to be sent at every sampling instant. These two factors would consume more network resources and thus further aggravate network congestion. In order to reduce the data transmission times in the feedback channel of each agent, an event-triggering mode is an alternative choice [23,24]. Especially in [25–28], the cooperative control problems for NMASs based on dynamic event triggering strategies were studied.

Therefore, in this paper, an event-triggered networked predictive control method is proposed for the cooperative output tracking problem of a linear heterogeneous NMAS with random network delays and packet dropouts in the feedback and forward channels of each agent. The main contributions of this paper are summarized as follows.

- (i) An event-triggering transmission mechanism is introduced in the feedback channel of each agent to reduce data transmission times. Furthermore, the state observer is placed at the plant side of each agent, and thus, only a single state estimate is needed to be transmitted to the controller. The effect of the network on the state estimates is eliminated.
- (ii) A novel cooperative output tracking predictive control protocol with proportional and integral actions is designed, where predicted system estimate increments and output tracking errors are used, and a necessary and sufficient condition is obtained for the stability of the resulting closed-loop system.
- (iii) Numerical simulation is carried out for an NMAS consisting of three DC motor systems, and four cases of simulation results are provided and compared, which illustrate the effectiveness of the proposed control scheme.

**Notation 1.**  $\mathbb{R}^n$  and  $\mathbb{R}^{n \times q}$  represent the  $n$ -dimensional Euclidean space and the set of real matrices with dimension  $n \times q$ , respectively. The superscript “ $T$ ” stands for the transposition of a matrix.  $\text{diag}\{\cdot\}$  denotes a diagonal matrix.

## 2. Control Scheme

In NMASs, graph theory is generally used as a tool to analyze them, and the communication topology between NMASs can be modeled as a directed graph  $P = (\kappa, \varepsilon, \zeta)$ , in which each agent is seen as a node. The symbol  $\kappa = \{1, 2, \dots, N\}$  represents a collection of all nodes, the symbol  $\varepsilon \in (\varepsilon_{ij}, i, j = 1, 2, \dots, N, i \neq j)$  denotes the communication channel between nodes  $i$  and  $j$ , and the symbol  $\zeta = [a_{i,j}]$  is the adjacency matrix of  $P$ , where  $a_{i,j} = 1$  if agent  $i$  can receive the data from agent  $j$ ; otherwise,  $a_{i,j} = 0$ .

A leader-following linear heterogeneous NMAS is considered, which consists of one leader agent and  $N - 1$  following agents. The communication topology of the system is symmetric and shown in Figure 1. Each agent is a linear discrete-time system as follows:

$$\begin{cases} x_i(k+1) = A_i x_i(k) + B_i u_i(k) \\ y_i(k) = C_i x_i(k), \end{cases} \quad (1)$$

where  $x_i(k) \in \mathbb{R}^n$ ,  $u_i(k) \in \mathbb{R}^m$ , and  $y_i(k) \in \mathbb{R}^q$  are the system state, control input, and system output of agent  $i$ , respectively;  $A_i$ ,  $B_i$ , and  $C_i$  are matrices with suitable dimensions;  $i \in \{1, 2, \dots, N\}$  is the mark of agents. It is assumed that  $(A_i, B_i)$  is controllable, and  $(A_i, C_i)$  is observable. Agent 1 and the remaining agents are defined as the leader agent and the following agents, respectively.

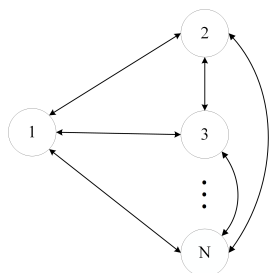


Figure 1. Communication topology.

Suppose that there exist random network delays and packet dropouts in the feedback (sensor-to-controller) and forward (controller-to-actuator) channels of each agent. It is assumed that the sensor, controller, and actuator of each agent system are time-driven and synchronous, and the packets transmit through networks with timestamps. By using the way described in [29], the two-channel network delays and packet dropouts are uniformly treated as random time delays of each channel, which are denoted by  $\tau_{k,i}^{sc}$  and  $\tau_{k,i}^{ca}$ , respectively. It is assumed that  $0 \leq \tau_{k,i}^{sc} \leq \bar{\tau}_i^{sc}$  and  $0 \leq \tau_{k,i}^{ca} \leq \bar{\tau}_i^{ca}$ , where  $\bar{\tau}_i^{sc}$  and  $\bar{\tau}_i^{ca}$  are all positive integers. Our purpose is to track the reference signal  $z(k) \in \mathbb{R}^q$  and make the output tracking error of each agent  $e_i(k) \rightarrow 0$ , where

$$e_i(k) = z_i(k) - y_i(k), \tag{2}$$

$$z_i(k) = \begin{cases} r(k), & i = 1, \\ y_1(k), & i \neq 1, \end{cases} \tag{3}$$

where  $r(k)$  is the reference signal of the leader agent.

To achieve the aforementioned purpose, an event-triggered networked cooperative predictive control scheme is designed, as shown in Figure 2. The state observer is performed as

$$\hat{x}_i(k+1|k) = A_i \hat{x}_i(k|k-1) + B_i u_i(k) + \tilde{L}_i (y_i(k) - C_i \hat{x}_i(k|k-1)), \tag{4}$$

where  $\tilde{L}_i \in \mathbb{R}^{n \times q}$  is the observer gain to be determined, and it can be designed by the pole assignment method.

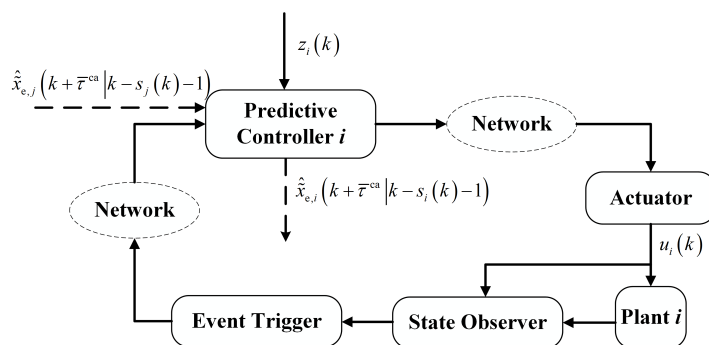


Figure 2. Event-triggered networked cooperative predictive control.

For the sake of the reduction of unnecessary packet transmission in the feedback channel, an event-triggered mechanism is used, and the triggering condition is given as

$$T_{i,\varphi+1} = \min\{k | (\hat{x}_i(k) - \hat{x}_i(T_{i,\varphi}))^T \Omega_i (\hat{x}_i(k) - \hat{x}_i(T_{i,\varphi})) > \eta_i \hat{x}_i(k)^T \Omega_i \hat{x}_i(k)\}, \tag{5}$$

where  $T_{i,\varphi}$  is the last triggering instant of agent  $i$ ,  $\hat{x}_i(k)$  denotes  $\hat{x}_i(k|k-1)$ ,  $0 < \eta_i < 1$  is a scalar, and  $\Omega_i > 0$  is a positive definite matrix. Furthermore, in order to avoid the case that the trigger is not triggered for a long time, it is required that  $T_{\varphi+1} \leq T_{\varphi} + W_i$ , where  $W_i$  is the maximum triggering interval. When condition (5) is satisfied, the state

estimate  $\hat{x}_i(k|k-1)$  is transmitted to the predictive controller via the feedback channel; otherwise,  $\hat{x}_i(k|k-1)$  is not transmitted so as to save network resources. It is obvious that an additional time delay will be introduced by the event trigger, which is denoted by  $\tau_{k,i}^e \leq W_i$ . The total time delay in the feedback channel is defined as  $s_i(k)$ , where  $s_i(k) = \tau_{k,i}^{sc} + \tau_{k,i}^e$ , and  $0 \leq s_i(k) \leq \bar{s}_i$  with  $\bar{s}_i = \bar{\tau}_i^{sc} + W_i$ .

In the predictive controller, when the delayed state estimate  $\hat{x}_i(k-s_i(k)|k-s_i(k)-1)$  is received, the predictions of the system state can be obtained based on (1):

$$\begin{aligned} \hat{x}_i(k-s_i(k)+v_i|k-s_i(k)-1) &= A_i \hat{x}_i(k-s_i(k)+v_i-1|k-s_i(k)-1) \\ &\quad + B_i u_i(k-s_i(k)+v_i-1), \end{aligned} \tag{6}$$

for  $v_i = 1, 2, \dots, s_i(k) + \bar{\tau}^{ca}$  with  $\bar{\tau}^{ca} = \max\{\bar{\tau}_i^{ca}\}$ . Then, the prediction of the output tracking error is obtained based on (2) as

$$\hat{e}_i(k + \bar{\tau}^{ca} | k - s_i(k) - 1) = \hat{z}_i(k + \bar{\tau}^{ca} | k - s_1(k) - 1) - \hat{y}_i(k + \bar{\tau}^{ca} | k - s_i(k) - 1), \tag{7}$$

where

$$\hat{z}_i(k + \bar{\tau}^{ca} | k - s_1(k) - 1) = \begin{cases} r(k + \bar{\tau}^{ca}), & i = 1, \\ \hat{y}_1(k + \bar{\tau}^{ca} | k - s_1(k) - 1), & i \neq 1, \end{cases} \tag{8}$$

$$\hat{y}_i(k + \bar{\tau}^{ca} | k - s_i(k) - 1) = C_i \hat{x}_i(k + \bar{\tau}^{ca} | k - s_i(k) - 1). \tag{9}$$

Then, the following incremental control law is designed:

$$\begin{aligned} \Delta u_i(k + \bar{\tau}^{ca}) &= -K_i^a \hat{x}_{e,i}(k + \bar{\tau}^{ca} | k - s_i(k) - 1) \\ &\quad + K_i^b \sum_{j=1, j \neq i}^N a_{i,j} (\hat{x}_{e,j}(k + \bar{\tau}^{ca} | k - s_j(k) - 1) - \hat{x}_{e,i}(k + \bar{\tau}^{ca} | k - s_i(k) - 1)), \end{aligned} \tag{10}$$

where  $K_i^a \in \mathbb{R}^{m \times (n+q)}$  and  $K_i^b \in \mathbb{R}^{m \times (n+q)}$  are controller gain matrices, and  $\hat{x}_{e,i}(k + \bar{\tau}^{ca} | k - s_i(k) - 1) = [\Delta \hat{x}_i(k + \bar{\tau}^{ca} | k - s_i(k) - 1)^T \hat{e}_i(k + \bar{\tau}^{ca} | k - s_i(k) - 1)^T]^T$ . Thus, the future control input at time  $k + \bar{\tau}^{ca}$  is

$$u_i(k + \bar{\tau}^{ca}) = u_i(k + \bar{\tau}^{ca} - 1) + \Delta u_i(k + \bar{\tau}^{ca}). \tag{11}$$

In order to compensate the random time delays in the feedback and forward channels of each agent, at each time instant, the predictive controller sends the control prediction sequence  $U_i(k + \bar{\tau}^{ca}) = [u_i^T(k), u_i^T(k+1), \dots, u_i^T(k + \bar{\tau}^{ca})]^T$  and its timestamp to the actuator. Based on the latest control prediction sequence available in the actuator, the  $(\tau_{k,i}^{ca} + 1)$ -th control signal is applied to the controlled plant.

**Remark 1.** The first novelty of this paper is that two-channel random communication constraints of each agent are considered simultaneously, and then, they are separately compensated according to their different features (see (6)). That is, the feedback channel delay  $s_i(k)$ , including the adverse effect of the event trigger introduced, can be accurately obtained in the predictive controller and thus is real-time compensated. Since the forward channel delay  $\tau_{k,i}^{ca}$  cannot be calculated in advance, it is compensated according to its upper bound.

**Remark 2.** The second novelty of this paper lies in the design of cooperative control protocol (10). It is easy to see that the first term of (10) is used to make  $y_1(k)$  track  $r(k)$  and  $y_i(k)$  ( $i \neq 1$ ) track  $y_1(k)$ , and the second term is used to achieve the cooperative output consensus of the NMAS. Furthermore, with the usage of  $\hat{x}_{e,i}(k + \bar{\tau}^{ca} | k - s_i(k) - 1) = [\Delta \hat{x}_i(k + \bar{\tau}^{ca} | k - s_i(k) - 1)^T \hat{e}_i(k + \bar{\tau}^{ca} | k - s_i(k) - 1)^T]^T$ , the control law is the combination of proportional and integral actions.

**Remark 3.** The selection of  $W_i$  is determined by the precision of the available model of each agent. In practice, a certain plant–model mismatch is inevitable. It can be seen from (6) that with the plant–model mismatch, a large delay would lead to a large state prediction error and then affect the system performance. In the total delay  $s_i(k) + \bar{\tau}^{ca}$ , only the impact of the event trigger, i.e.,  $\tau_{k,i}^e$ , can be tuned as needed by choosing  $W_i$ . Therefore, considering the trade-off of saving network resource and prediction accuracy, a large value of  $W_i$  can be chosen for a high model accuracy and vice versa.

### 3. Stability Analysis

In this section, the stability of the closed-loop NMAS is analyzed. Without loss of generality, let the reference signal  $r(\cdot) = 0$ .

From (4), we have

$$\hat{x}_i(k + 1|k) = A_i\hat{x}_i(k|k - 1) + B_iu_i(k) + \tilde{L}_iC_i\vartheta_i(k), \tag{12}$$

where  $\vartheta_i(k) = x_i(k) - \hat{x}_i(k|k - 1)$ . Subtracting (12) from (1) leads to

$$\vartheta_i(k + 1) = (A_i - \tilde{L}_iC_i)\vartheta_i(k). \tag{13}$$

It is obtained from (6) that

$$\hat{x}_i(k|k - \tau_{k,i} - 1) = A_i^{\tau_{k,i}}\hat{x}_i(k - \tau_{k,i}|k - \tau_{k,i} - 1) + \sum_{j=1}^{\tau_{k,i}} A_i^{j-1}B_iu_i(k - j), \tag{14}$$

where  $\tau_{k,i} = s_i(k - \bar{\tau}^{ca}) + \bar{\tau}^{ca}$ ,  $0 \leq \tau_{k,i} \leq \bar{\tau}_i$ , and  $\bar{\tau}_i = \bar{s}_i + \bar{\tau}^{ca}$ . It follows from (1) that

$$x_i(k) = A_i^{\tau_{k,i}}x_i(k - \tau_{k,i}) + \sum_{j=1}^{\tau_{k,i}} A_i^{j-1}B_iu_i(k - j). \tag{15}$$

Subtracting (14) from (15) yields

$$x_i(k) - \hat{x}_i(k|k - \tau_{k,i} - 1) = A_i^{\tau_{k,i}}\vartheta_i(k - \tau_{k,i}). \tag{16}$$

From (1), we have

$$\begin{aligned} \Delta x_i(k) &= A_i\Delta x_i(k - 1) + B_i\Delta u_i(k - 1) \\ &= A_i^{\tau_{k,i}-1}\Delta x_i(k - \tau_{k,i} + 1) + \sum_{j=1}^{\tau_{k,i}-1} A_i^{j-1}B_i\Delta u_i(k - j). \end{aligned} \tag{17}$$

From (6), we obtain

$$\Delta \hat{x}_i(k|k - \tau_{k,i} - 1) = A_i^{\tau_{k,i}-1}\Delta \hat{x}_i(k - \tau_{k,i} + 1|k - \tau_{k,i} - 1) + \sum_{j=1}^{\tau_{k,i}-1} A_i^{j-1}B_i\Delta u_i(k - j). \tag{18}$$

By using (1), (6), and (16), subtracting (18) from (17) gives

$$\begin{aligned} \Delta x_i(k) - \Delta \hat{x}_i(k|k - \tau_{k,i} - 1) &= A_i^{\tau_{k,i}-1} \left( \Delta x_i(k - \tau_{k,i} + 1) - \Delta \hat{x}_i(k - \tau_{k,i} + 1|k - \tau_{k,i} - 1) \right) \\ &= A_i^{\tau_{k,i}-1} \left( A_i x_i(k - \tau_{k,i}) + B_i u_i(k - \tau_{k,i}) \right. \\ &\quad \left. - x_i(k - \tau_{k,i}) - A_i \hat{x}_i(k - \tau_{k,i}|k - \tau_{k,i} - 1) \right. \\ &\quad \left. - B_i u_i(k - \tau_{k,i}) + \hat{x}_i(k - \tau_{k,i}|k - \tau_{k,i} - 1) \right) \\ &= A_i^{\tau_{k,i}-1} (A_i - I) \left( x_i(k - \tau_{k,i}) - \hat{x}_i(k - \tau_{k,i}|k - \tau_{k,i} - 1) \right) \\ &= A_i^{\tau_{k,i}-1} (A_i - I) \vartheta_i(k - \tau_{k,i}). \end{aligned} \tag{19}$$

By subtracting (7) from (2), we obtain

$$e_1(k) - \hat{e}_1(k|k - \tau_{k,1}) = -C_1 A_1^{\tau_{k,1}} \vartheta_1(k - \tau_{k,1}), \tag{20}$$

$$e_i(k) - \hat{e}_i(k|k - \tau_{k,i}) = C_1 A_1^{\tau_{k,1}} \vartheta_1(k - \tau_{k,1}) - C_i A_i^{\tau_{k,i}} \vartheta_i(k - \tau_{k,i}), \quad i \neq 1. \tag{21}$$

From (10), we have

$$\begin{aligned} \Delta u_i(k) = & -K_i^a \hat{x}_{e,i}(k|k - \tau_{k,i} - 1) + K_i^b \sum_{j=1, j \neq i}^N a_{i,j} (\hat{x}_{e,j}(k|k - \tau_{k,j} - 1) \\ & - \hat{x}_{e,i}(k|k - \tau_{k,i} - 1)). \end{aligned} \tag{22}$$

From (1) and (2), we get

$$\begin{cases} x_{e,i}(k+1) = \tilde{A}_{e,i} x_{e,i}(k) + \tilde{B}_{e,i} \Delta u_i(k) + \tilde{E}_e \Delta z_i(k+1) \\ \Delta y_i(k) = \tilde{C}_{e,i} x_{e,i}(k), \end{cases} \tag{23}$$

where

$$\begin{aligned} x_{e,i}(k) = & \begin{bmatrix} \Delta x_i(k) \\ e_i(k) \end{bmatrix}, \quad \tilde{A}_{e,i} = \begin{bmatrix} A_i & 0 \\ -C_i A_i & I \end{bmatrix}, \\ \tilde{B}_{e,i} = & \begin{bmatrix} B_i \\ -C_i B_i \end{bmatrix}, \quad \tilde{C}_{e,i} = \begin{bmatrix} C_i^T \\ 0 \end{bmatrix}^T, \quad \tilde{E}_e = \begin{bmatrix} 0 \\ I \end{bmatrix}. \end{aligned}$$

From (19), (20), and (21), we have

$$x_{e,1}(k) - \hat{x}_{e,1}(k|k - \tau_{k,1} - 1) = G_1 \vartheta_1(k - \tau_{k,1}), \tag{24}$$

$$x_{e,i}(k) - \hat{x}_{e,i}(k|k - \tau_{k,i} - 1) = H_i \vartheta_i(k - \tau_{k,i}) + G_2 \vartheta_1(k - \tau_{k,1}), \quad i \neq 1, \tag{25}$$

where

$$G_1 = \begin{bmatrix} A_1^{\tau_{k,1}-1} (A_1 - I) \\ -C_1 A_1^{\tau_{k,1}} \end{bmatrix}, \quad G_2 = \begin{bmatrix} 0 \\ C_1 A_1^{\tau_{k,1}} \end{bmatrix}, \quad H_i = \begin{bmatrix} A_i^{\tau_{k,i}-1} (A_i - I) \\ -C_i A_i^{\tau_{k,i}} \end{bmatrix}, \quad i \neq 1.$$

For  $i = 1$ , substituting (22) into the first equation of (23) gives

$$\begin{aligned} x_{e,1}(k+1) = & \tilde{A}_{e,1} x_{e,1}(k) + \tilde{B}_{e,1} (-K_1^a \hat{x}_{e,1}(k|k - \tau_{k,1} - 1) \\ & + K_1^b \sum_{j=1, j \neq 1}^N a_{1,j} (\hat{x}_{e,j}(k|k - \tau_{k,j} - 1) - \hat{x}_{e,1}(k|k - \tau_{k,1} - 1))) \\ = & (\tilde{A}_{e,1} - \tilde{B}_{e,1} d_1) x_{e,1}(k) + \tilde{B}_{e,1} \sum_{j=2}^N f_{1,j} x_{e,j}(k) \\ & + \tilde{B}_{e,1} (K_1^a G_1 + \sum_{j=2}^N f_{1,j} (G_1 - G_2)) \vartheta_1(k - \tau_{k,1}) - \tilde{B}_{e,1} \sum_{j=2}^N f_{1,j} H_j \vartheta_j(k - \tau_{k,j}), \end{aligned} \tag{26}$$

where  $d_1 = K_1^a + \sum_{j=2}^N f_{1,j}$ , and  $f_{1,j} = K_1^b a_{1,j}$ . Substituting (26) into the second equation of (23) leads to

$$\begin{aligned} \Delta y_1(k+1) = & \tilde{C}_{e,1} (\tilde{A}_{e,1} - \tilde{B}_{e,1} d_1) x_{e,1}(k) + \tilde{C}_{e,1} \tilde{B}_{e,1} \sum_{j=2}^N f_{1,j} x_{e,j}(k) \\ & + \tilde{C}_{e,1} \tilde{B}_{e,1} (K_1^a G_1 + \sum_{j=2}^N f_{1,j} (G_1 - G_2)) \vartheta_1(k - \tau_{k,1}) \end{aligned}$$

$$- \tilde{C}_{e,1} \tilde{B}_{e,1} \sum_{j=2}^N f_{1,j} H_j \vartheta_j(k - \tau_{k,j}). \tag{27}$$

For  $i \neq 1$ , from (22), (23), and (27), we have

$$\begin{aligned} x_{e,i}(k+1) &= (\tilde{A}_{e,i} - \tilde{B}_{e,i} d_i + \tilde{E}_e \tilde{C}_{e,1} \tilde{B}_{e,1} f_{1,i}) x_{e,i}(k) \\ &+ (\tilde{E}_e \tilde{C}_{e,1} (\tilde{A}_{e,1} - \tilde{B}_{e,1} d_1) + \tilde{B}_{e,i} f_{i,1}) x_{e,1}(k) \\ &+ \sum_{j=2, j \neq i}^N (\tilde{B}_{e,i} f_{i,j} + \tilde{E}_e \tilde{C}_{e,1} \tilde{B}_{e,1} f_{1,j}) x_{e,j}(k) \\ &+ \tilde{C}_{e,1} \tilde{B}_{e,1} (K_1^a G_1 + \sum_{j=2}^N f_{1,j} (G_1 - G_2)) \vartheta_1(k - \tau_{k,1}) \\ &- \tilde{C}_{e,1} \tilde{B}_{e,1} \sum_{j=2}^N f_{1,j} H_j \vartheta_j(k - \tau_{k,j}) + \tilde{B}_{e,i} d_i H_i \vartheta_i(k - \tau_{k,i}) \\ &- \tilde{B}_{e,i} \sum_{j=1, j \neq i}^N f_{i,j} H_j \vartheta_j(k - \tau_{k,j}) + \tilde{B}_{e,i} K_i^a G_2 \vartheta_1(k - \tau_{k,1}), \end{aligned} \tag{28}$$

where  $d_i = K_i^a + \sum_{j=2}^N f_{i,j}$ , and  $f_{i,j} = K_i^b a_{i,j}$ .

Thus, from (13), (26), and (28), we obtain the following closed-loop system:

$$X(k+1) = \Phi X(k), \tag{29}$$

where

$$\begin{aligned} X(k) &= \begin{bmatrix} X_{e,i}(k) \\ \tilde{\vartheta}(k) \end{bmatrix}, \quad \Phi = \begin{bmatrix} \Gamma & \omega(k) \\ 0 & \Lambda \end{bmatrix}, \quad X_{e,i}(k) = [x_{e,1}(k)^T \ x_{e,2}(k)^T \ \dots \ x_{e,N}(k)^T]^T, \\ \tilde{\vartheta}(k) &= [\tilde{\vartheta}_1(k)^T \ \tilde{\vartheta}_2(k)^T \ \dots \ \tilde{\vartheta}_N(k)^T]^T, \quad \tilde{\vartheta}_i(k) = [\vartheta_i(k)^T \ \vartheta_i(k-1)^T \ \dots \ \vartheta_i(k-\bar{\tau}_i)^T]^T. \\ \Gamma &= \begin{bmatrix} \tilde{A}_{e,1} - \tilde{B}_{e,1} d_1 & \tilde{B}_{e,1} f_{1,2} & \dots \\ \tilde{E}_e \tilde{C}_{e,1} (\tilde{A}_{e,1} - \tilde{B}_{e,1} d_1) + \tilde{B}_{e,2} f_{2,1} & \tilde{A}_{e,2} - \tilde{B}_{e,2} d_2 + \tilde{E}_e \tilde{C}_{e,1} \tilde{B}_{e,1} f_{1,2} & \dots \\ \vdots & \vdots & \dots \\ \tilde{E}_e \tilde{C}_{e,1} (\tilde{A}_{e,1} - \tilde{B}_{e,1} d_1) + \tilde{B}_{e,N} f_{N,1} & \tilde{B}_{e,N} f_{N,2} + \tilde{E}_e \tilde{C}_{e,1} \tilde{B}_{e,1} f_{1,2} & \dots \\ & \tilde{B}_{e,1} f_{1,N} \\ & \tilde{B}_{e,2} f_{2,N} + \tilde{E}_e \tilde{C}_{e,1} \tilde{B}_{e,1} f_{1,N} \\ & \vdots \\ & \tilde{A}_{e,N} - \tilde{B}_{e,N} d_N + \tilde{E}_e \tilde{C}_{e,1} \tilde{B}_{e,1} f_{1,N} \end{bmatrix}, \\ \Lambda &= \text{diag} \left\{ \underbrace{A_1 - \tilde{L}_1 C_1, \dots, A_1 - \tilde{L}_1 C_1}_{\bar{\tau}_1+1}, \dots, \underbrace{A_N - \tilde{L}_N C_N, \dots, A_N - \tilde{L}_N C_N}_{\bar{\tau}_N+1} \right\}. \end{aligned}$$

From (29), we know that the matrix  $\Phi$  is an upper triangular matrix, where time-varying matrix  $\omega(k)$  is not related to the stability of the closed-loop system and thus is omitted here. Therefore, we have the following theorem.

**Theorem 1.** *The closed-loop NMAS (29) is asymptotically stable if and only if the eigenvalues of the matrices  $\Gamma$  and  $\Lambda$  are within the unit circle.*

#### 4. Simulation Results

In this section, we use the actual models of three DC motor systems for numerical simulation to verify the effectiveness of the proposed method. The sampling period of the three motor systems is 0.05 s, and the model parameters are identified as follows:

$$\begin{aligned} A_1 &= \begin{bmatrix} 1.18 & -0.145 \\ 2 & 0 \end{bmatrix}, B_1 = \begin{bmatrix} 4 \\ 0 \end{bmatrix}, C_1 = [ 4.24 \quad 2.67 ], \\ A_2 &= \begin{bmatrix} 1.38 & -0.102 \\ 2 & 0 \end{bmatrix}, B_2 = \begin{bmatrix} 4 \\ 0 \end{bmatrix}, C_2 = [ 4.94 \quad 2.68 ], \\ A_3 &= \begin{bmatrix} 1.20 & -0.147 \\ 2 & 0 \end{bmatrix}, B_3 = \begin{bmatrix} 4 \\ 0 \end{bmatrix}, C_3 = [ 4.002 \quad 2.30 ]. \end{aligned}$$

Using the pole assignment method, the gain matrices of the observer (4) for the three motors respectively are

$$\tilde{L}_1 = \begin{bmatrix} 0.0434 \\ 0.1116 \end{bmatrix}, \tilde{L}_2 = \begin{bmatrix} 0.0336 \\ 0.0831 \end{bmatrix}, \tilde{L}_3 = \begin{bmatrix} 0.0614 \\ 0.1538 \end{bmatrix}.$$

The controller gain matrices in (10) are chosen as

$$\begin{aligned} K_1^a &= [ 0.2116 \quad -0.0325 \quad -0.0068 ], \\ K_2^a &= [ 0.2427 \quad -0.0249 \quad -0.0063 ], \\ K_3^a &= [ 0.2947 \quad -0.0332 \quad -0.0140 ], \\ K_1^b &= [ 0.0001 \quad 0.0001 \quad 0.0001 ], \\ K_2^b &= [ 0.00135 \quad 0.0315 \quad 0.00018 ], \\ K_3^b &= [ 0.0005 \quad 0.0001 \quad 0.0001 ]. \end{aligned}$$

The communication topology is deployed with  $a_{1,1} = a_{2,2} = a_{3,3} = 0, a_{2,1} = a_{3,1} = a_{1,2} = a_{1,3} = a_{2,3} = a_{3,2} = 1$ . In addition, random network delays in the feedback and forward channels are chosen as  $\tau_{k,i}^{sc} \in [2 \ 5]$  and  $\tau_{k,i}^{ca} \in [2 \ 6]$ . The parameters of the three event triggers are given as  $W_1 = 10, W_2 = 13, W_3 = 16, \eta_1 = \eta_2 = \eta_3 = 0.01$ , and  $\Omega_1 = \Omega_2 = \Omega_3 = I$ .

For comparison, the following four simulation cases are considered.

Case 1 (without delays): In this case, the communication in the NMAS is ideal, and the event trigger is not used. The simulation result is shown in Figure 3. It can be seen from Figure 3 that all the three motors have good output tracking control performance.

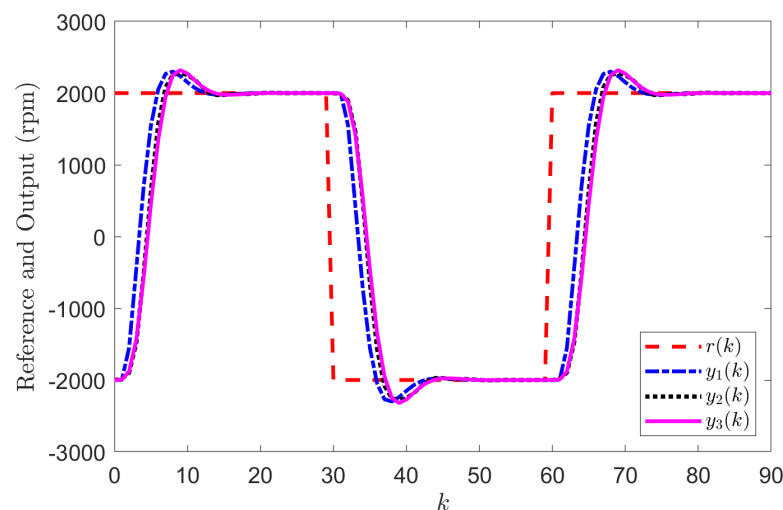


Figure 3. Simulation result of Case 1.

Case 2 (with delays but without compensation): In this case, random network delays  $\tau_{k,i}^{sc} \in [2\ 5]$  and  $\tau_{k,i}^{ca} \in [2\ 6]$  are considered, but the proposed delay compensation scheme is not used. The simulation result is given in Figure 4. It is clear from Figure 4 that the random network delays lead to the instability of the closed-loop NMAS.

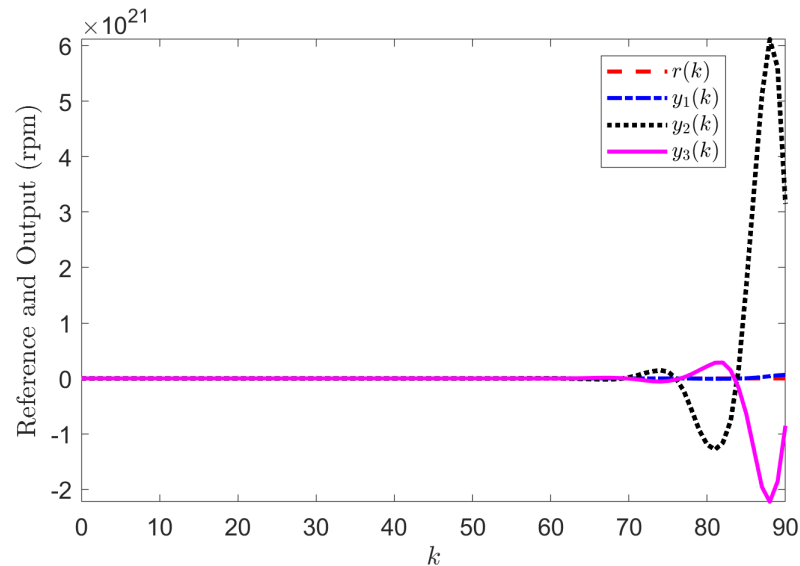


Figure 4. Simulation result of Case 2.

Case 3 (with delays and with compensation): This case considers the same random network delays as in Case 2, and they are actively compensated by the proposed scheme. The simulation result is shown in Figure 5. It can be seen that from Figure 5 that the control performance is greatly improved compared with Figure 4, which even approaches the performance of local control case without network delays in Case 1. Furthermore, zero steady-state output tracking errors are also achieved.

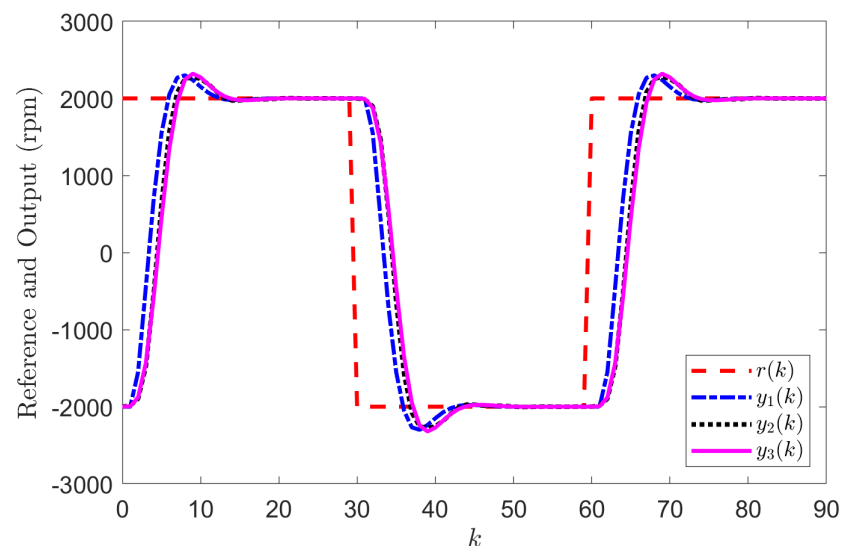
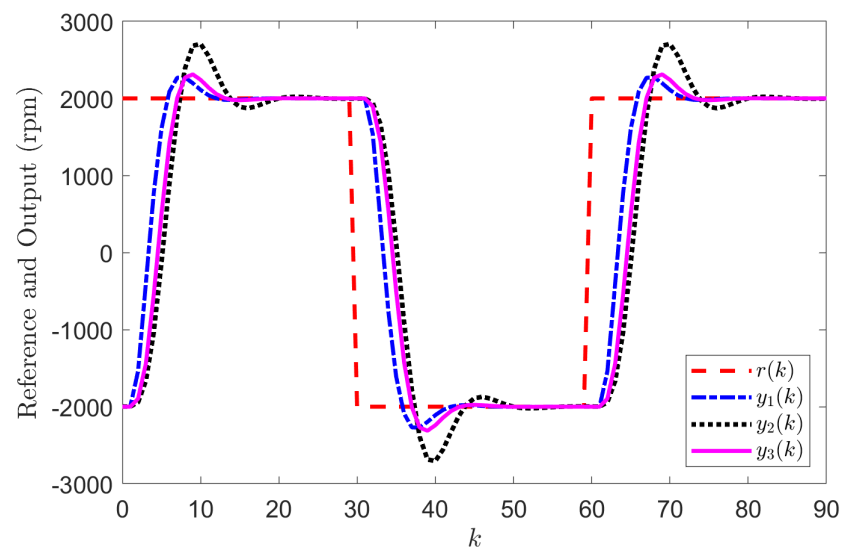


Figure 5. Simulation result of Case 3.

Case 4 (with delays and compensation but without coordination): In this case, the same network environment as in Cases 2 and 3 is considered, and the proposed compensation scheme is used, but the second term of the control law (10) is not used, i.e.,  $K_1^b = K_2^b = K_3^b = [0\ 0\ 0]$ . The output responses of the three motors are shown in Figure 6. It is obvious that agents 2 and 3 have poor coordination performance.



**Figure 6.** Simulation result of Case 4.

To show the effect of the event trigger, the network delay and the total time delay in the feedback channel, i.e.,  $\tau_i^{sc}(k)$  and  $s_i(k)$ , are given in Figure 7, and the triggering instants are shown in Figure 8 for the simulation result of the proposed method in Figure 5, where “1(0)” means that the event trigger is (not) triggered. It can be seen from Figure 8 that among the 90 sampling instants, the event triggers of agents 1, 2, and 3 are triggered 24 times and 66 packets are not transmitted, which leads to the total time delay  $s_i(k)$  far greater than the original network delays  $\tau_i^{sc}(k)$  (see Figure 7), but the cooperative output tracking performance is not affected under the proposed compensation scheme. Furthermore, since a large amount of packets are not transmitted, the network resources of the NMAS are largely saved.

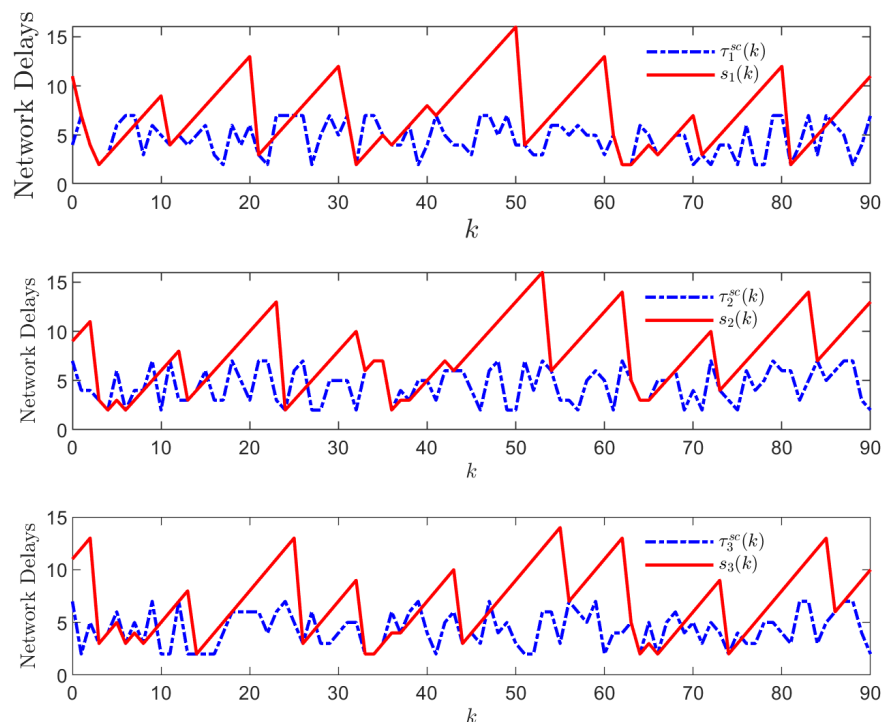


**Figure 7.**  $\tau_i^{sc}(k)$  and  $s_i(k)$  for  $i = 1, 2, 3$ .

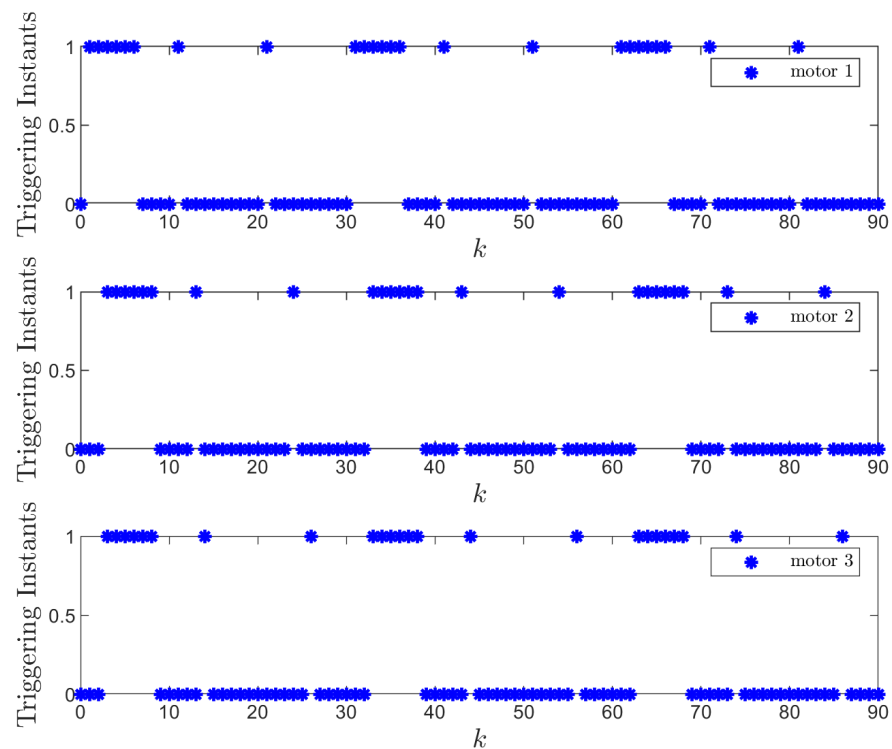


Figure 8. Triggering instants of motors 1, 2, and 3.

## 5. Conclusions

In this paper, an event-triggered cooperative output tracking predictive control scheme has been proposed for a class of linear heterogeneous NMASs with random network delays and packet dropouts in both the feedback and forward channels of each agent, and these communication constraints can be actively compensated. At the same time, the introduction of an event-triggering transmission mechanism and a state observer placed at the plant side have greatly saved the network resources of each feedback channel. The effectiveness of the proposed scheme has been demonstrated by the simulation results of cooperative control of three motor systems. In our future work, the secure control issues of NMASs subject to sensor/actuator faults and cyber attacks as well as random communication constraints will be further investigated [30–33], although they are more challenging.

**Author Contributions:** Conceptualization, C.L.; Formal analysis, T.D.; Funding acquisition, Z.P.; Investigation, T.D. and C.L.; Methodology, Z.P.; Supervision, Z.P. and C.L.; Validation, T.D. and C.Z.; Visualization, C.Z.; Writing—original draft, T.D.; Writing—review & editing, Z.P. All authors have read and agreed to the published version of the manuscript.

**Funding:** This research was funded by National Natural Science Foundation of China under Grant 62173002, Beijing Natural Science Foundation under Grant 4222045, Youth Talent Support Program of Beijing Municipality, and NCUT Yujie Talent Training Program.

**Institutional Review Board Statement:** Not applicable.

**Informed Consent Statement:** Not applicable.

**Data Availability Statement:** Not applicable.

**Conflicts of Interest:** The authors declare no conflict of interest.

## References

1. Liu, G.-P.; Zhang, S. A survey on formation control of small satellites. *Proc. IEEE* **2018**, *106*, 440–457. [[CrossRef](#)]
2. Liu, Y.; Montenbruck, J.M.; Zelazo, D.; Odelga, M.; Rajappa, S.; Bühlhoff, H.H.; Allgöwer, F. A distributed control approach to formation balancing and maneuvering of multiple multirotor UAVs. *IEEE Trans. Rob.* **2018**, *34*, 870–882. [[CrossRef](#)]

3. Saradagi, A.; Muralidharan, V.; Krishnan, V.; Menta, S.; Mahindrakar, A.D. Formation control and trajectory tracking of nonholonomic mobile robots. *IEEE Trans. Control Syst. Technol.* **2018**, *26*, 2250–2258. [[CrossRef](#)]
4. Su, Y. Output feedback cooperative control for linear uncertain multiagent systems with nonidentical relative degrees. *IEEE Trans. Autom. Control* **2016**, *61*, 4027–4033. [[CrossRef](#)]
5. Liu, T.; Huang, J. Adaptive cooperative output regulation of discrete-time linear multi-agent systems by a distributed feedback control law. *IEEE Trans. Autom. Control* **2018**, *63*, 4383–4390. [[CrossRef](#)]
6. Han, T.; Zheng, W.X. Bipartite output consensus for heterogeneous multi-agent systems via output regulation approach. *IEEE Trans. Circuits Syst. II Express Briefs* **2021**, *68*, 281–285. [[CrossRef](#)]
7. Pang, Z.-H.; Zheng, C.-B.; Sun, J.; Han, Q.-L.; Liu, G.-P. Distance-and velocity-based collision avoidance for time-varying formation control of second-order multi-agent systems. *IEEE Trans. Circuits Syst. II Express Briefs* **2021**, *68*, 1253–1257. [[CrossRef](#)]
8. Hong, H.; Wang, H. Fixed-time formation control for second-order disturbed multi-agent systems under directed graph. *Symmetry* **2021**, *13*, 2295. [[CrossRef](#)]
9. Liu, G.-P. Coordinated control of networked multiagent systems via distributed cloud computing using multistep state predictors. *IEEE Trans. Cybern.* **2022**, *52*, 810–820. [[CrossRef](#)] [[PubMed](#)]
10. Pang, Z.-H.; Zheng, C.-B.; Li, C.; Liu, G.-P.; Han, Q.-L. Cloud-based time-varying formation predictive control of multi-agent systems with random communication constraints and quantized signals. *IEEE Trans. Circuits Syst. II Express Briefs* **2021**. [[CrossRef](#)]
11. Liu, Z.; Yan, W.; Li, H.; Small, M. Cooperative output regulation problem of multi-agent systems with stochastic packet dropout and time-varying communication delay. *J. Franklin Inst.* **2018**, *355*, 8664–8682. [[CrossRef](#)]
12. Yang, Y.; Zhang, X.-M.; He, W.; Han, Q.-L.; Peng, C. Sampled-position states based consensus of networked multi-agent systems with second-order dynamics subject to communication delays. *Inf. Sci.* **2020**, *509*, 36–46. [[CrossRef](#)]
13. Shariati, A.; Zhao, Q. Robust leader-following output regulation of uncertain multi-agent systems with time-varying delay. *IEEE/CAA J. Autom. Sin.* **2018**, *5*, 807–817. [[CrossRef](#)]
14. Ma, L.; Wang, Y.-L.; Han, Q.-L.  $H_\infty$  cluster formation control of networked multiagent systems with stochastic sampling. *IEEE Trans. Cybern.* **2021**, *51*, 5761–5772. [[CrossRef](#)]
15. Liu, G.-P. Predictive control of networked multiagent systems via cloud computing. *IEEE Trans. Cybern.* **2017**, *47*, 1852–1859. [[CrossRef](#)]
16. An, B.-R.; Liu, G.-P.; Tan, C. Group consensus control for networked multi-agent systems with communication delays. *ISA Trans.* **2018**, *76*, 78–87. [[CrossRef](#)] [[PubMed](#)]
17. Tan, C.; Yin, X.; Liu, G.-P.; Huang, J.; Zhao, Y.-B. Prediction-based approach to output consensus of heterogeneous multi-agent systems with delays. *IET Control Theory Appl.* **2018**, *12*, 20–28. [[CrossRef](#)]
18. Liu, Z.-Q.; Wang, Y.-L.; Wang, T.-B. Incremental predictive control-based output consensus of networked unmanned surface vehicle formation systems. *Inf. Sci.* **2018**, *457*, 166–181. [[CrossRef](#)]
19. Tan, C.; Yue, L.; Li, Y.; Liu, G.-P. Group consensus control for discrete-time heterogeneous multi-agent systems with time delays. *Neurocomputing* **2020**, *392*, 70–85. [[CrossRef](#)]
20. Chen, D.-L.; Liu, G.-P. A networked predictive controller for linear multi-agent systems with communication time delays. *J. Frankl. Inst.* **2020**, *357*, 9442–9446. [[CrossRef](#)]
21. Yang, H.; Ju, S.; Xia, Y.; Zhang, J. Predictive cloud control for networked multiagent systems with quantized signals under DoS attacks. *IEEE Trans. Syst. Man Cybern. Syst.* **2021**, *51*, 1345–1353. [[CrossRef](#)]
22. Pang, Z.-H.; Luo, W.-C.; Liu, G.-P.; Han, Q.-L. Observer-based incremental predictive control of networked multi-agent systems with random delays and packet dropouts. *IEEE Trans. Circuits Syst. II Express Briefs* **2021**, *68*, 426–430. [[CrossRef](#)]
23. Qi, W.; Zong, G.; Zheng, W. Adaptive event-triggered SMC for stochastic switching systems with semi-Markov process and application to boost converter circuit model. *IEEE Trans. Circuits Syst. I Regul. Pap.* **2021**, *68*, 786–796. [[CrossRef](#)]
24. Jin, Y.; Qi, W.; Zong, G. Finite-time synchronization of delayed semi-Markov neural networks with dynamic event-triggered scheme. *Int. J. Control Autom. Syst.* **2021**, *19*, 2297–2308. [[CrossRef](#)]
25. Nowzari, C.; Garcia, E.; Cortés, J. Event-triggered communication and control of networked systems for multi-agent consensus. *Automatica* **2019**, *105*, 1–27. [[CrossRef](#)]
26. Yi, X.; Liu, K.; Dimarogonas, D.V.; Johansson, K.H. Dynamic event-triggered and self-triggered control for multi-agent systems. *IEEE Trans. Autom. Control* **2019**, *64*, 3300–3307. [[CrossRef](#)]
27. He, W.; Xu, B.; Han, Q.-L.; Qian, F. Adaptive consensus control of linear multiagent systems with dynamic event-triggered strategies. *IEEE Trans. Cybern.* **2020**, *50*, 2996–3008. [[CrossRef](#)] [[PubMed](#)]
28. Hu, W.; Yang, C.; Huang, T.; Gui, W. A distributed dynamic event-triggered control approach to consensus of linear multiagent systems with directed networks. *IEEE Trans. Cybern.* **2020**, *50*, 869–874. [[CrossRef](#)]
29. Pang, Z.; Bai, C.; Liu, G.; Han, Q.; Zhang, X. A novel networked predictive control method for systems with random communication constraints. *J. Syst. Sci. Complex.* **2021**, *34*, 1364–1378. [[CrossRef](#)]
30. Pang, Z.-H.; Xia, C.-G.; Zhai, W.-F.; Liu, G.-P.; Han, Q.-L. Networked active fault-tolerant predictive control for systems with random communication constraints and actuator/sensor faults. *IEEE Trans. Circuits Syst. II Express Briefs* **2021**. [[CrossRef](#)]
31. Pang, Z.-H.; Fan, L.-Z.; Sun, J.; Liu, K.; Liu, G.-P. Detection of stealthy false data injection attacks against networked control systems via active data modification. *Inf. Sci.* **2021**, *546*, 192–205. [[CrossRef](#)]

32. Pang, Z.-H.; Fan, L.-Z.; Dong, Z.; Han, Q.-L.; Liu, G.-P. False data injection attacks against partial sensor measurements of networked control systems. *IEEE Trans. Circuits Syst. II Express Briefs* **2022**, *69*, 149–153. [[CrossRef](#)]
33. Mustafa, A.; Modares, H. Attack analysis and resilient control design for discrete-time distributed multi-agent systems. *IEEE Rob. Autom. Lett.* **2020**, *5*, 369–376. [[CrossRef](#)]